X-636-63-197

25p.

N64-16032

CODE-1

(NASA TMX-54604)

DERIVATION AND GENERAL CALCULATION OF CONSERVATIVE TORQUES EXERTED AT THE PADDLE-ARM AXIS OF A LABORATORY MODEL SATELLITE AND THE DETERMINATION OF THE MOMENT OF INERTIA ABOUT THE PADDLE-ARM AXIS OF A RECTANGULAR SOLAR PADDLE WITH VARIABLE PITCH

SEPTEMBER 1963

auth. #1

NASA

GODDARD SPACE FLIGHT CENTER

GREENBELT, MD.

16032

SUMMARY

In an effort to provide design data for the construction of an electromechanical system with the two degrees of freedom required for solar paddle orientation, the following expressions were determined: (1) the total conservative torque acting at the paddle-arm-rotation axis as a function of geometry and paddle-arm angle, and (2) the moment of inertia about the paddle-arm-rotation axis for a rectangular solar paddle as a function of geometry and pitch angle. The appendices include examples of determining the paddle-arm angles at which equilibrium and maximum conservative torques occur, data tables, and curves of the derived expressions for a specific geometry. AUTHOR

DERIVATION AND GENERAL CALCULATION OF CONSERVATIVE TORQUES EXERTED AT THE PADDLE-ARM AXIS OF A LABORATORY MODEL SATELLITE AND THE DETERMINATION OF THE MOMENT OF INERTIA ABOUT THE PADDLE-ARM AXIS OF A RECTANGULAR SOLAR PADDLE WITH VARIABLE PITCH

by

S. G. McCarron Sep. 1963 orig

Goddard Space Flight Center, Greenbelt, Maryland

INTRODUCTION

To date, spin-stabilized satellites powered by solar paddles generally have stationary paddles. As a spin-stabilized satellite travels around the sun, the angle between the spin axis and sun line continually changes (except for the special case where the sun line is always normal to the spin axis) because the spin axis is fixed in space. In addition, torques resulting from atmospheric drag, magnetic-field gradient, solar pressure, etc., cause the sun-line spin-axis angle to undergo changes after launching. For a particular satellite, shadowing occurs in a specific part of the sun-line spin-axis range of angle. That is, the body of the satellite shades the solar paddles or the solar paddles shadow one another. In order to improve a particular solar-paddle aspect ratio when shadowing occurs, a system was devised in which two non-adjacent solar paddles (out of a total of four) are allowed two degrees of freedom. Two ideal degrees of freedom would be: (1) movement about the paddle-arm-rotation axis, and (2) movement about the longitudinal axis of the paddle. The orientation system of the model satellite being built within the Space Power Technology Branch is to eventually incorporate those degrees of freedom, and to have the adjustable paddle arms move in a 180-degree out-of-phase fashion when shadowing occurs. A further development of such a system could be variable solar-paddle aspect ratio at any sun-line spin-axis angle; this could maintain the charging rate as solar cell degradation occurs, or decrease the charging rate as the battery system becomes charged. The present system under construction is an intermittent duty one, whereas future systems will be continuous duty.

CONSERVATIVE TORQUES

The total conservative torque acting at the fulcrum of a solar-paddle arm (on a model satellite) is composed of centrifugal and gravitational components. The centrifugal torque results from the spin of the satellite and the fact that the center of mass of the paddle does not lie at the paddle-arm-rotation axis. The gravitational torque arises from the fact that gravity acts near the geometrical center of the paddle, which lies off the paddle-arm-rotation axis. The nonconservative torques which arise from frictional forces are neglected in the calculations.

Figure 1 shows an IMP-type satellite with two of the four rectangular solar paddles movable. The geometry of the satellite is labeled as follows: (1) R is the radius of the satellite, (2) λ is the length of a paddle arm, (3) a is the width of a paddle, (4) b is the length of a paddle, (5) c is the thickness of a paddle, (6) θ is the subtended paddle-arm

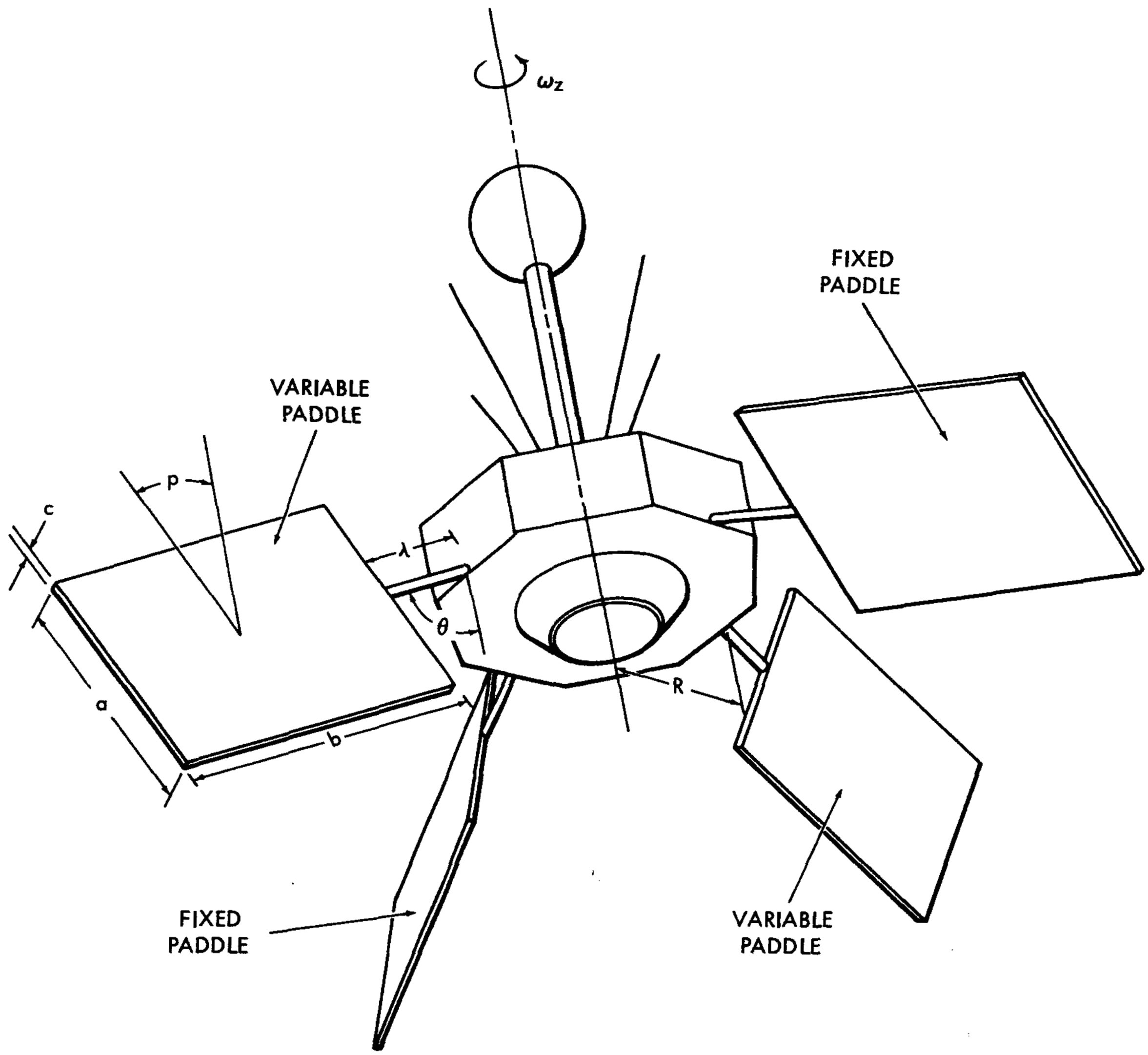

Figure 1. An IMP-type satellite, whose configuration was used in designing the laboratory satellite, is shown with the variable rectangular solar paddles.

angle, (7) p is the paddle-pitch angle, and (8) ω_z is the angular velocity* about the spin axis of the figure. Figure 2 shows a schematic diagram of the conservative torques acting at the paddle-arm-rotation axis. The total conservative torque acting at the fulcrum of the paddle arm at an angle θ to the vertical is given by

*The model is being driven by a constant speed motor, thus making ω_z constant.

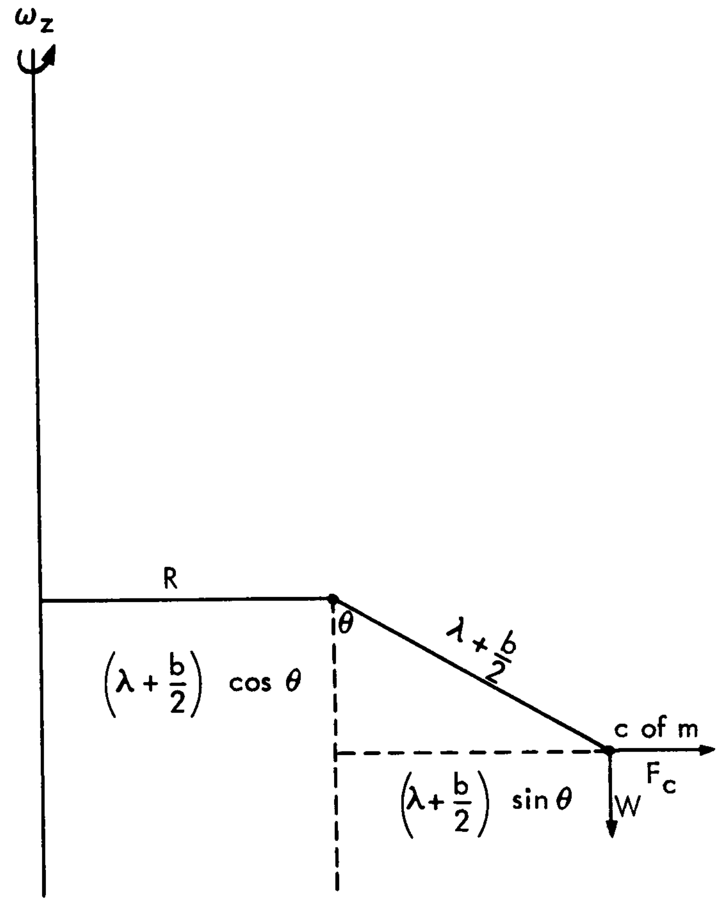

Figure 2. A schematic diagram of the conservative torques acting at the paddle-arm-rotation axis of the laboratory model.

$$\sum_{i=1}^{2} M_i = F_c \left(\lambda + \frac{b}{2}\right) \cos\theta - W \left(\lambda + \frac{b}{2}\right) \sin\theta \tag{1}$$

where F_c is the centrifugal force given by

$$F_c = m\left[R + \left(\lambda + \frac{b}{2}\right) \sin\theta\right]\omega_z^2 = \frac{W}{g}\left[R + \left(\lambda + \frac{b}{2}\right) \sin\theta\right]\omega_z^2 \tag{2}$$

and W is the weight given by

$$W = mg \tag{3}$$

where m is the mass of the paddle and g is the acceleration due to gravity. Substituting equations (2) and (3) into equation (1) gives

$$\sum_{i=1}^{2} M_i = W\left(\lambda + \frac{b}{2}\right)\left\{\frac{\omega_z^2}{g}\left[R\cos\theta + \left(\lambda + \frac{b}{2}\right)\frac{\sin 2\theta}{2}\right] - \sin\theta\right\} \tag{4}$$

The equilibrium condition is given by

$$\sum_{i=1}^{2} M_i = 0; \quad \frac{\omega_z^2}{g}\left[R\cos\theta + \left(\lambda + \frac{b}{2}\right)\frac{\sin 2\theta}{2}\right] - \sin\theta = 0 \tag{5}$$

Reducing equation (5) to terms containing powers of $\sin\theta$ gives

$$\left(\lambda + \frac{b}{2}\right)^2 \omega_z^4 \sin^4\theta + 2R \left(\lambda + \frac{b}{2}\right) \omega_z^4 \sin^3\theta$$

$$+ \left[R^2 \omega_z^4 - \left(\lambda + \frac{b}{2}\right)^2 \omega_z^4 + g^2\right] \sin^2\theta$$

$$- 2R \left(\lambda + \frac{b}{2}\right) \omega_z^4 \sin\theta - R^2 \omega_z^4 = 0 \qquad (6)$$

Appendix I gives a solution of equation (6) for the case of the model satellite under development. Horner's method is used to approximate the desired root of equation (6) with the determined coefficients.

The derivative of equation (4) gives

$$\frac{d}{d\theta}\left[\sum_{i=1}^{2} M_i\right] = W \left(\lambda + \frac{b}{2}\right) \left\{\frac{\omega_z^2}{g} \left[-R \sin\theta + \left(\lambda + \frac{b}{2}\right)\cos 2\theta\right] - \cos\theta\right\} \qquad (7)$$

Maxima and minima are obtained from the equation

$$\frac{d}{d\theta}\left[\sum_{i=1}^{2} M_i\right] = 0 \qquad (8)$$

Reducing equation (8) to terms containing powers of $\sin\theta$ gives

$$4\omega_z^4\left(\lambda+\frac{b}{2}\right)^2\sin^4\theta+4R\omega_z^4\left(\lambda+\frac{b}{2}\right)\sin^3\theta$$

$$+\left[\omega_z^4 R^2-4\omega_z^4\left(\lambda+\frac{b}{2}\right)^2+g^2\right]\sin^2\theta$$

$$-2R\omega_z^4\left(\lambda+\frac{b}{2}\right)\sin\theta+\omega_z^4\left(\lambda+\frac{b}{2}\right)^2-g^2=0 \qquad (9)$$

Appendix II gives a solution of equation (9) for the case of the model satellite under development. Again Horner's method is used to approximate the desired root.

The general torque equation is normalized by rearranging the terms of equation (4)

$$\frac{\Sigma M_i}{W\left(\lambda+\frac{b}{2}\right)}=R\omega_z^2\left[\frac{\cos\theta}{g}\right]+\left(\lambda+\frac{b}{2}\right)\omega_z^2\left[\frac{\sin 2\theta}{2g}\right]+\left[-\sin\theta\right] \qquad (10)$$

Let

$$f_1=R\omega_z^2\left[\frac{\cos\theta}{g}\right] \qquad (11a)$$

$$f_2=\left(\lambda+\frac{b}{2}\right)\omega_z^2\left[\frac{\sin 2\theta}{2g}\right] \qquad (11b)$$

$$f_3=\left[-\sin\theta\right] \qquad (11c)$$

Normalizing equations (11) with respect to the geometrical parameters and spin rate gives

$$\frac{f_1}{R\omega_z^2} = \left[\frac{\cos\theta}{g}\right] \tag{12a}$$

$$\frac{f_2}{\left(\lambda + \frac{b}{2}\right)\omega_z^2} = \left[\frac{\sin 2\theta}{2g}\right] \tag{12b}$$

$$f_3 = \left[-\sin\theta\right] \tag{12c}$$

Each right hand side of equations (12) is plotted in Figure 3. The value of f_3 and the normalized values of f_1 and f_2 are determined from the curves for each particular θ. Denormalizing each amplitude factor and algebraically adding them gives the total normalized torque. Denormalizing again gives the total torque for a particular value of θ. A specific example for the model satellite is given in Appendix III. Figure 6 in Appendix III shows a plot of the total torque as a function of θ, for the model satellite.

MOMENT OF INERTIA

Figure 4 shows an isolated solar paddle drawn with respect to the paddle-arm uv-rotation plane. The geometry of the paddle, as labeled, refers to the translated-rotated $u''v''w''$ coordinate system. Coordinates in the $u'v'w'$ system are related to the coordinates in the $u''v''w''$ system by the following transformations:

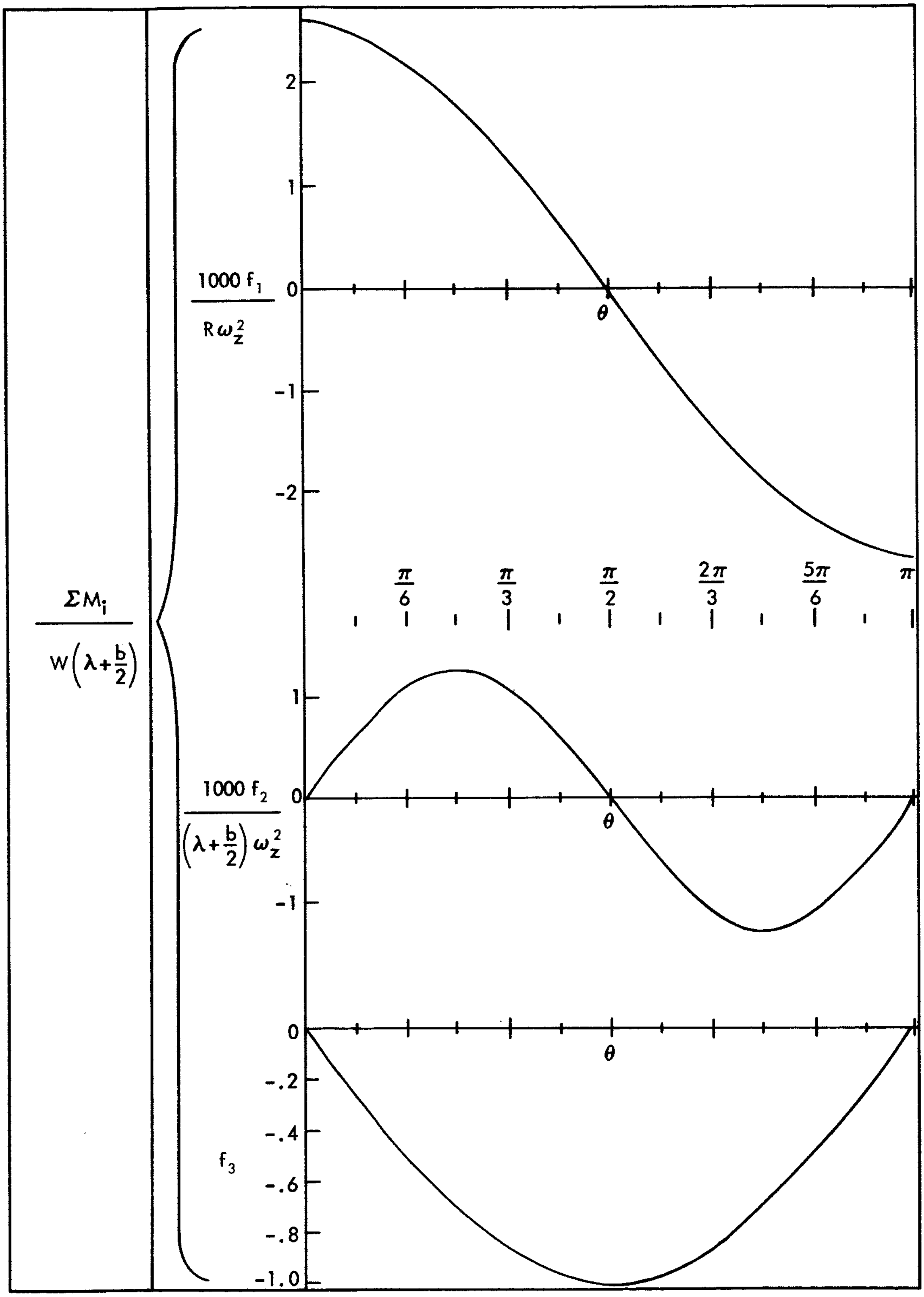

Figure 3. A graph of the normalized components of the general torque equation versus paddle-arm angle.

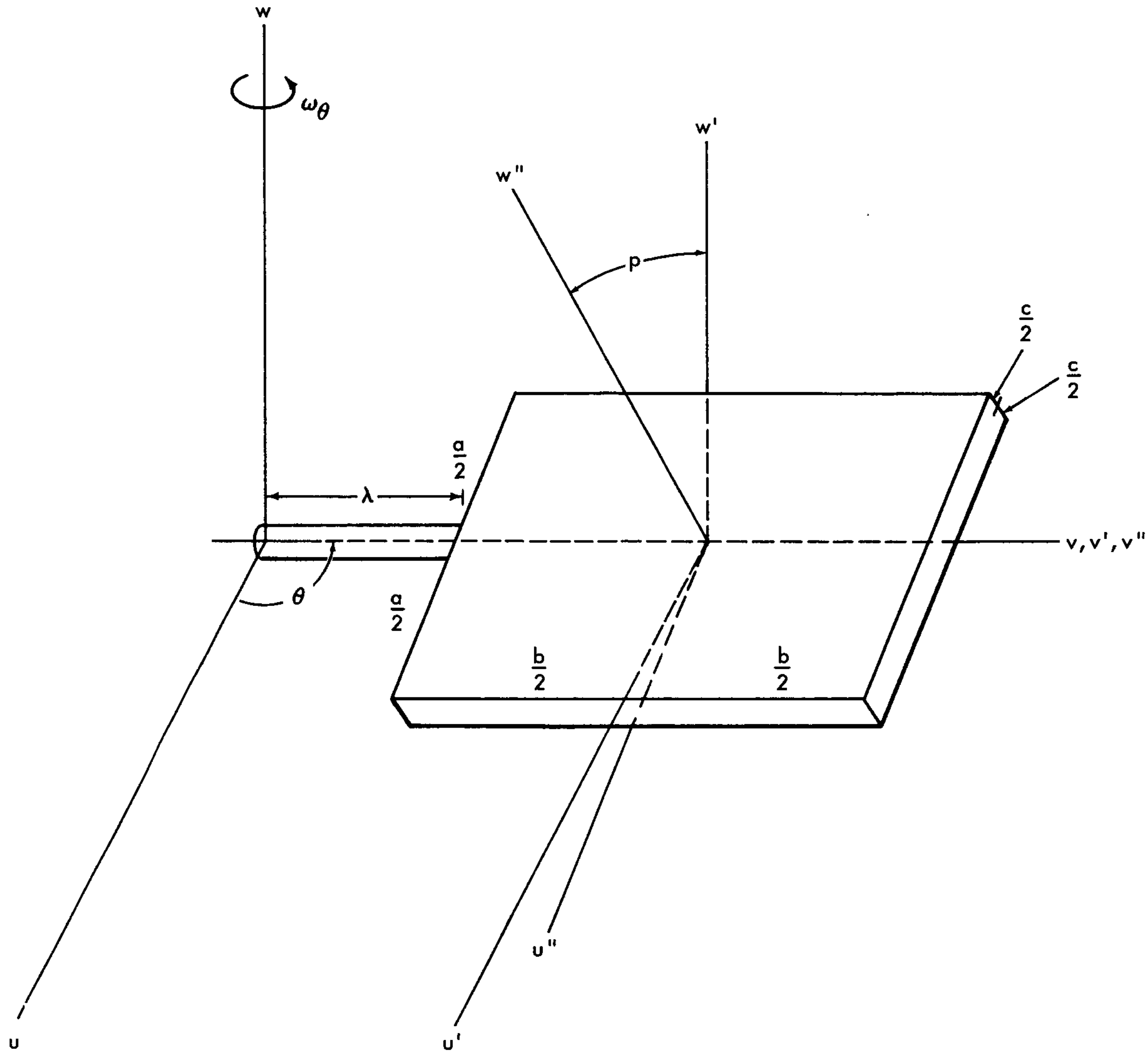

Figure 4. An isolated solar paddle drawn with respect to the paddle-arm uv-rotation plane.

$$\left.\begin{aligned} u' &= w'' \sin p + u'' \cos p \\ v' &= v'' \\ w' &= w'' \cos p - u'' \sin p \end{aligned}\right\} \qquad (13)$$

where p is the pitch angle of the paddle. The moment of inertia about the w'-axis of the u'v'w' coordinate system is by definition

$$I_{w'w'} = \int_m (u'^2 + v'^2)\, dm \tag{14}$$

Using the transformation equations (13), the above equation becomes

$$I_{w'w'} = \int_m (\sin^2 p\, w''^2 + \cos^2 p\, u''^2 + \sin 2p\, u''w'' + v''^2)\, dm \tag{15}$$

or

$$I_{w'w'} = \rho \int_{-\frac{c}{2}}^{\frac{c}{2}} \int_{-\frac{b}{2}}^{\frac{b}{2}} \int_{-\frac{a}{2}}^{\frac{a}{2}} (\sin^2 p\, w''^2 + \cos^2 p\, u''^2 + \sin 2p\, u''w'' + v''^2)\, du''\, dv''\, dw'' \tag{16}$$

where

$$dm = \rho\, du''\, dv''\, dw'' \tag{17}$$

Integrating over w'' gives

$$I_{w'w'} = \rho \int_{-\frac{b}{2}}^{\frac{b}{2}} \int_{-\frac{a}{2}}^{\frac{a}{2}} \left(\frac{c^3}{12} \sin^2 p + c \cos^2 p\, u''^2 + c\, v''^2\right) du''\, dv'' \tag{18}$$

Integrating over u'' gives

$$I_{w'w'} = \rho \int_{-\frac{b}{2}}^{\frac{b}{2}} \left(\frac{ac^3}{12} \sin^2 p + \frac{a^3 c}{12} \cos^2 p + acv''^2\right) dv'' \tag{19}$$

Integrating over v'' gives

$$I_{w'w'} = m \left(\frac{a^2}{12} \cos^2 p + \frac{b^2}{12} + \frac{c^2}{12} \sin^2 p \right) \tag{20}$$

where

$$m = \rho \, abc \tag{21}$$

Coordinates in the uvw system are related to the coordinates in the $u'v'w'$ system by the following transformations:

$$\left.\begin{aligned} u &= u' \\ v &= v' + \left(\lambda + \frac{b}{2}\right) \\ w &= w' \end{aligned}\right\} \tag{22}$$

where λ is the length of the paddle arm. The moment of inertia about the w-axis of the uvw coordinate system is by definition

$$I_{ww} = \int_m (u^2 + v^2) \, dm \tag{23}$$

substituting equations (22) in equation (23) gives

$$I_{ww} = \int_m (u'^2 + v'^2) \, dm + \left(\lambda + \frac{b}{2}\right)^2 \int_m dm + 2 \left(\lambda + \frac{b}{2}\right) \int_m v' \, dm \tag{24}$$

Integrating the above expression, the third term reduces to zero because of symmetry and the result is

$$I_{ww} = I_{w'w'} + \left(\lambda + \frac{b}{2}\right)^2 m \tag{25}$$

or

$$I = I_{ww} = m\left[\frac{a^2}{12}\cos^2 p + \frac{b^2}{12} + \frac{c^2}{12}\sin^2 p + \left(\lambda + \frac{b}{2}\right)^2\right] \tag{26}$$

The moment of inertia equation is normalized by writing it in the following form:

$$\frac{I}{m} = \frac{(a^2 - c^2)}{12}\left[\cos^2 p\right] + \left[\frac{b^2}{12} + \frac{c^2}{12} + \left(\lambda + \frac{b}{2}\right)^2\right] \tag{27}$$

Let

$$f_4 = \left(\frac{a^2 - c^2}{12}\right)\left[\cos^2 p\right] \tag{28a}$$

$$f_5 = \frac{b^2}{12} + \frac{c^2}{12} + \left(\lambda + \frac{b}{2}\right)^2 \tag{28b}$$

Normalizing equations (28) with respect to the geometrical parameters gives

$$\frac{f_4}{\frac{(a^2 - c^2)}{12}} = \left[\cos^2 p\right] \tag{29a}$$

$$\frac{f_5}{\frac{b^2}{12} + \frac{c^2}{12} + \left(\lambda + \frac{b}{2}\right)^2} = [1] \tag{29b}$$

Each right side of equations (29) is plotted in Figure 5. The normalized values of f_4 and f_5 are determined from the curves for each particular p. Denormalizing each amplitude factor and algebraically adding them gives the total normalized moment of inertia for a particular paddle-pitch angle. Denormalizing again gives the moment of inertia. A specific example for one of the model's paddles is given in Appendix IV. Figure 7 in Appendix IV shows a plot of the data obtained from Figure 5 for the particular paddle.

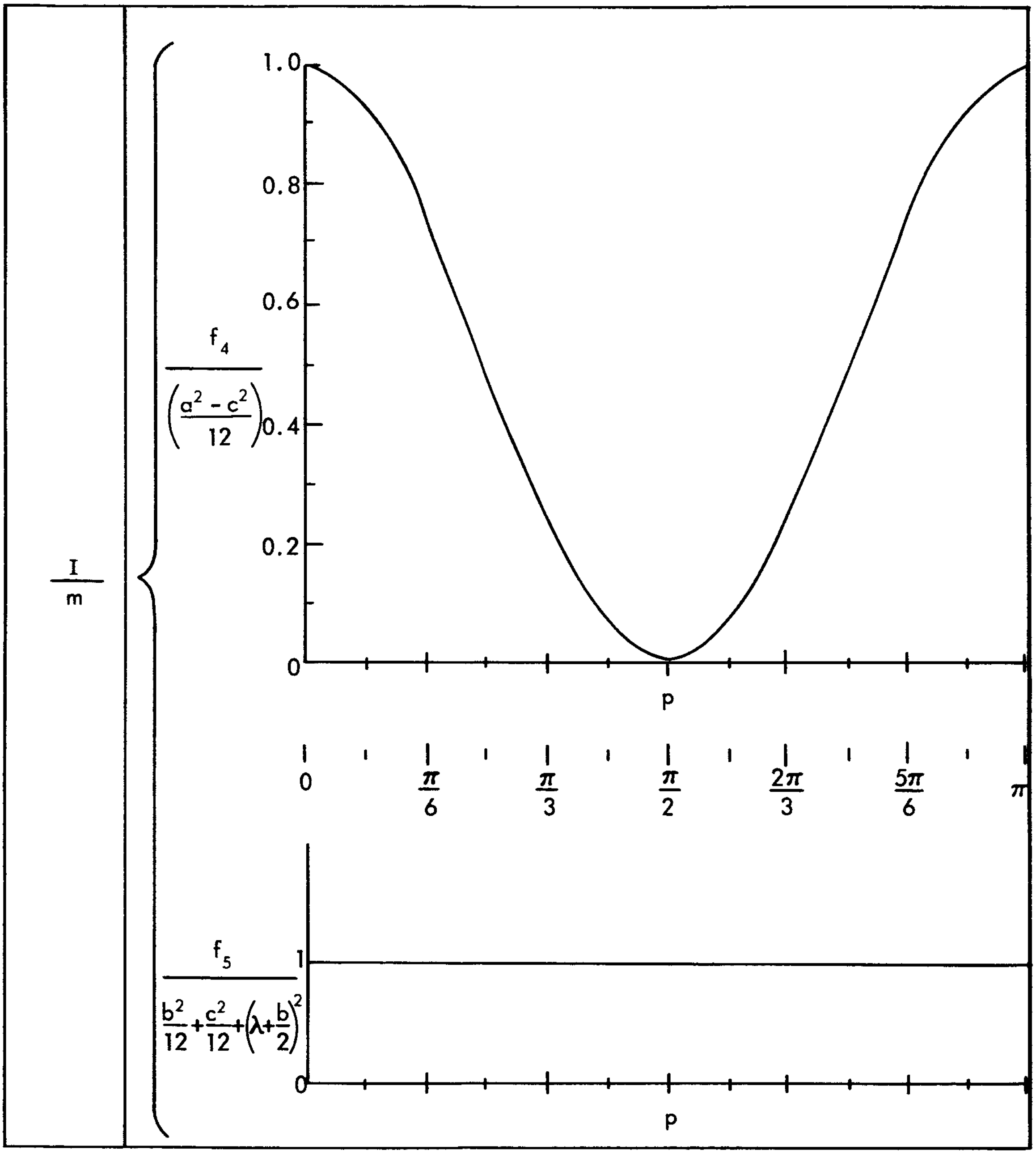

Figure 5. A graph of the normalized components of the paddle moment of inertia versus the paddle-pitch angle.

APPENDIX I

$a = 5.00$ in.	$\lambda = 2.25$ in.	$\omega_z = 2\pi$ rad-sec^{-1}
$b = 6.50$ in.	$R = 3.75$ in.	$g = 384$ in.-sec^{-2}

$$\left(\lambda+\frac{b}{2}\right)^2 \omega_z^4 \sin^4\theta + 2R\left(\lambda+\frac{b}{2}\right)\omega_z^4 \sin^3\theta$$

$$+\left[R^2\omega_z^4 - \left(\lambda+\frac{b}{2}\right)^2 \omega_z^4 + g^2\right]\sin^2\theta$$

$$- 2R\left(\lambda+\frac{b}{2}\right)\omega_z^4 \sin\theta - R^2\omega_z^4 = 0. \tag{6}$$

Evaluating the coefficients in the above equation gives

$$\left(\lambda+\frac{b}{2}\right)^2 \omega_z^4 = 0.472 \times 10^{-5} \text{ in.}^2\text{-sec}^{-4}$$

$$2R\left(\lambda+\frac{b}{2}\right)\omega_z^4 = 0.643 \times 10^{-5} \text{ in.}^2\text{-sec}^{-4}$$

$$R^2\omega_z^4 - \left(\lambda+\frac{b}{2}\right)^2 \omega_z^4 + g^2 = 1.22 \times 10^{-5} \text{ in.}^2\text{-sec}^{-4}$$

$$2R\left(\lambda+\frac{b}{2}\right)\omega_z^4 = 0.643 \times 10^{-5} \text{ in.}^2\text{-sec}^{-4}$$

$$R^2\omega_z^4 = 0.219 \times 10^{-5} \text{ in.}^2\text{-sec}^{-4}.$$

Substitution of calculated coefficients in quartic gives

$$\sin^4\theta + 1.36\sin^3\theta + 2.58\sin^2\theta - 1.36\sin\theta - 0.464 = 0$$

Horner's Method gives

1	1.36	2.58	-1.36	-0.464	0.5
	0.5	0.93	1.76	0.200	
1	1.86	3.51	0.40	-0.264	
	0.5	1.18	2.34		
1	2.36	4.69	2.74		
	0.5	1.43			
1	2.86	6.12			
	0.5				
1	3.36	6.12	2.74	-0.264	0.08
	0.08	0.27	0.51	0.260	
1	3.44	6.39	3.25	-0.004	
	0.08	0.28	0.53		
1	3.52	6.67	3.78		
	0.08	0.29			
1	3.60	6.96			
	0.08				
1	3.68	6.96	3.78	-0.004	0.001
	0.001	0.004	0.007	0.0038	
1	3.681	6.964	3.787	-0.0002	

$$\therefore \sin\theta = 0.5 + 0.08 + 0.001 + \cdots = 0.581^{+}$$
$$\theta = \arcsin(0.581)$$
$$\theta = 35.53^{\circ}$$

This is the angle at which equilibrium occurs.

APPENDIX II

$a = 5.00$ in. $\lambda = 2.25$ in. $\omega_z = 2\pi$ rad-sec^{-1}

$b = 6.50$ in. $R = 3.75$ in. $g = 384$ in.-sec^{-2}

$$4\omega_z^4 \left(\lambda+\frac{b}{2}\right)^2 \sin^4\theta + 4R\,\omega_z^4 \left(\lambda+\frac{b}{2}\right) \sin^3\theta$$

$$+ \left[\omega_z^4 R^2 - 4\omega_z^4 \left(\lambda+\frac{b}{2}\right)^2 + g^2\right] \sin^2\theta$$

$$- 2R\,\omega_z^4 \left(\lambda+\frac{b}{2}\right) \sin\theta + \omega_z^4 \left(\lambda+\frac{b}{2}\right)^2 - g^2 = 0. \qquad (9)$$

Evaluating the coefficients in the above equation gives

$$4\omega_z^4 \left(\lambda+\frac{b}{2}\right)^2 = 1.89 \times 10^{-5} \text{ in.}^2\text{-sec}^{-4}$$

$$4R\,\omega_z^4 \left(\lambda+\frac{b}{2}\right) = 1.29 \times 10^{-5} \text{ in.}^2\text{-sec}^{-4}$$

$$\omega_z^4 R^2 - 4\omega_z^4 \left(\lambda+\frac{b}{2}\right)^2 + g^2 = -0.193 \times 10^{-5} \text{ in.}^2\text{-sec}^{-4}$$

$$2R\,\omega_z^4 \left(\lambda+\frac{b}{2}\right) = 0.643 \times 10^{-5} \text{ in.}^2\text{-sec}^{-4}$$

$$\omega_z^4 \left(\lambda+\frac{b}{2}\right)^2 - g^2 = -1.00 \times 10^{-5} \text{ in.}^2\text{-sec}^{-4}.$$

Substitution of calculated coefficients in quartic gives

$$\sin^4\theta + 0.682 \sin^3\theta - 0.102 \sin^2\theta - 0.340 \sin\theta - 0.529 = 0$$

Horner's Method gives

1	0.682	-0.102	-0.340	-0.529	0.8
	0.8	1.186	0.867	0.422	
1	1.482	1.084	0.527	-0.107	
	0.8	1.826	2.328		
1	2.282	2.910	2.855		
	0.8	2.466			
1	3.082	5.376			
	0.8				
1	3.882	5.376	2.855	-0.107	0.03
	0.03	0.117	0.165	0.091	
1	3.912	5.493	3.020	-0.016	
	0.03	0.118	0.168		
1	3.942	5.611	3.188		
	0.03	0.119			
1	3.972	5.730			
	0.03				
1	4.002	5.730	3.188	-0.016	0.005
	0.005	0.020	0.029	0.0161	
1	4.007	5.750	3.217	+0.0001	

$$\therefore \sin\theta = 0.8 + 0.03 + 0.005 - \ldots = 0.835^{-}$$
$$\theta = \arcsin(0.835)$$
$$\theta = 123.38^\circ$$

This is the angle at which maximum torque occurs.

APPENDIX III

$a = 5.00$ in. $\qquad \omega_z = 2\pi$ rad-sec^{-1} $\qquad \frac{R\omega_z^2}{1000} = 0.148$ in.-sec^{-2}

$b = 6.50$ in. $\qquad W = 100$ gm-wt $= 3.53$ oz

$\lambda = 2.25$ in. $\qquad \lambda + \frac{b}{2} = 5.50$ in. $\qquad \frac{\left(\lambda+\frac{b}{2}\right)\omega_z^2}{1000} = 0.217$ in.-sec^{-2}

$R = 3.75$ in. $\qquad W\left(\lambda+\frac{b}{2}\right) = 19.4$ oz-in.

θ	$\frac{1000\,f_1}{R\omega_z^2}$	f_1	$\frac{1000\,f_2}{\left(\lambda+\frac{b}{2}\right)\omega_z^2}$	f_2	f_3	$f_1+f_2+f_3$	$W\left(\lambda+\frac{b}{2}\right)(f_1+f_2+f_3)$
0°	2.60	0.385	0.00	0.000	0.000	0.385	7.47
15°	2.51	0.371	0.65	0.141	-0.259	0.253	4.91
30°	2.25	0.333	1.13	0.245	-0.500	0.078	1.51
45°	1.84	0.272	1.30	0.282	-0.707	-0.153	- 2.97
60°	1.30	0.192	1.13	0.245	-0.866	-0.429	- 8.32
75°	0.67	0.099	0.65	0.141	-0.966	-0.726	-14.1
90°	0.00	0.000	0.00	0.000	-1.000	-1.000	-19.4
105°	-0.67	-0.099	-0.65	-0.141	-0.966	-1.21	-23.4
120°	-1.30	-0.192	-1.13	-0.245	-0.866	-1.30	-25.3
135°	-1.84	-0.272	-1.30	-0.282	-0.707	-1.26	-24.5
150°	-2.25	-0.333	-1.13	-0.245	-0.500	-1.08	-20.9
165°	-2.51	-0.371	-0.65	-0.141	-0.259	-0.771	-15.0
180°	-2.60	-0.385	0.00	0.000	0.000	-0.385	- 7.47

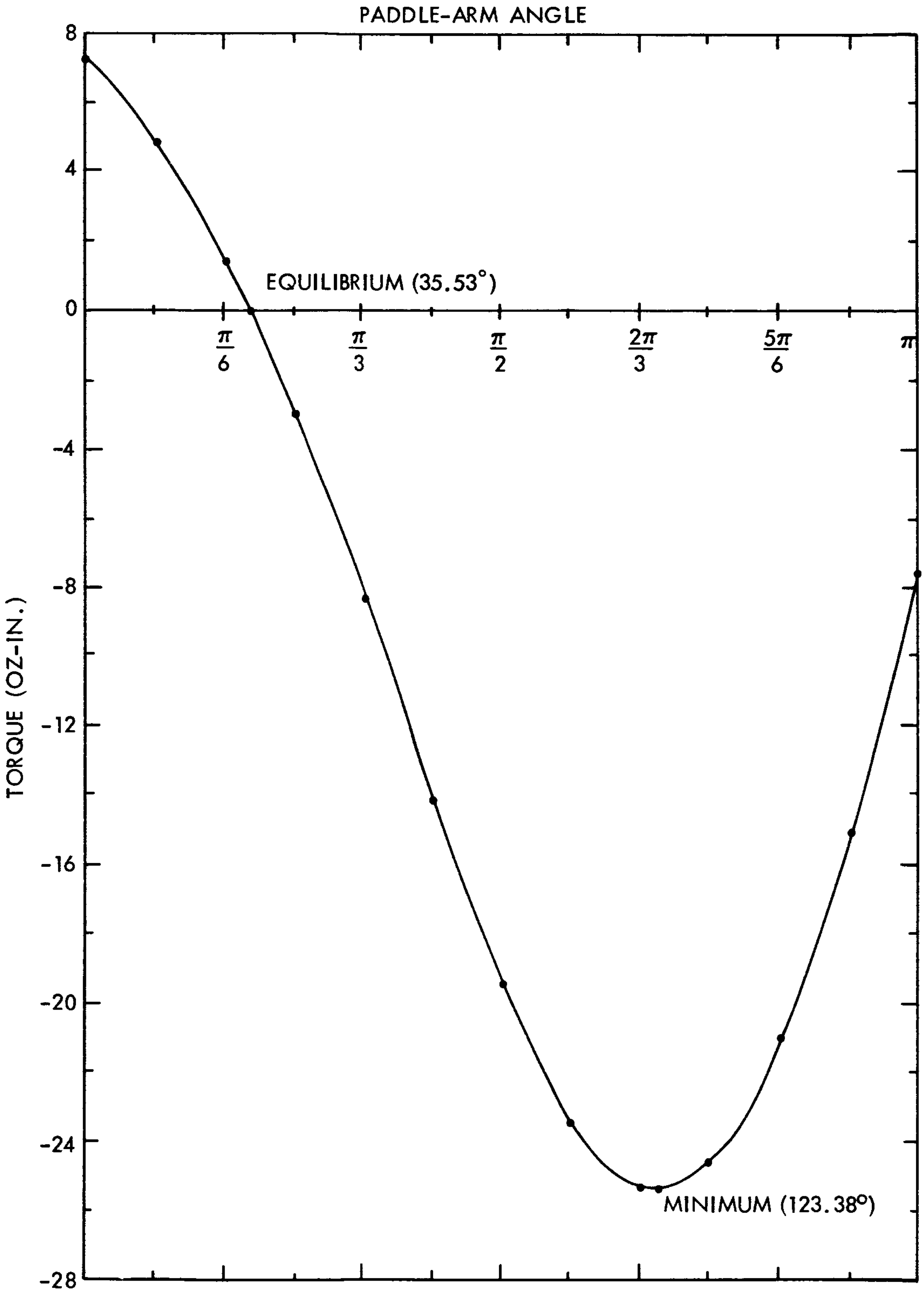

Figure 6. A plot of conservative torque versus paddle-arm angle for the model satellite.

APPENDIX IV

$a = 5.00$ in. $\qquad m = 6.89 \times 10^{-3}$ slugs $\qquad \dfrac{a^2 - c^2}{12} = 2.07$ in.^{2}

$b = 6.50$ in. $\qquad \lambda + \dfrac{b}{2} = 5.50$ in. $\qquad \dfrac{b^2}{12} + \dfrac{c^2}{12} + \left(\lambda + \dfrac{b}{2}\right)^2 = 33.8$ in.^{2}

$c = 0.375$ in.

p	$\dfrac{f_4}{\frac{(a^2 - c^2)}{12}}$	f_4	$f_4 + f_5$	$m(f_4 + f_5)$
0°	1.000	2.07	35.9	0.247
15°	0.933	1.93	35.7	0.246
30°	0.750	1.55	35.4	0.244
45°	0.500	1.04	34.8	0.240
60°	0.250	0.518	34.3	0.236
75°	0.067	0.139	33.9	0.234
90°	0.000	0.000	33.8	0.233
105°	0.067	0.139	33.9	0.234
120°	0.250	0.518	34.3	0.236
135°	0.500	1.04	34.8	0.240
150°	0.750	1.55	35.4	0.244
165°	0.933	1.93	35.7	0.246
180°	1.000	2.07	35.9	0.247

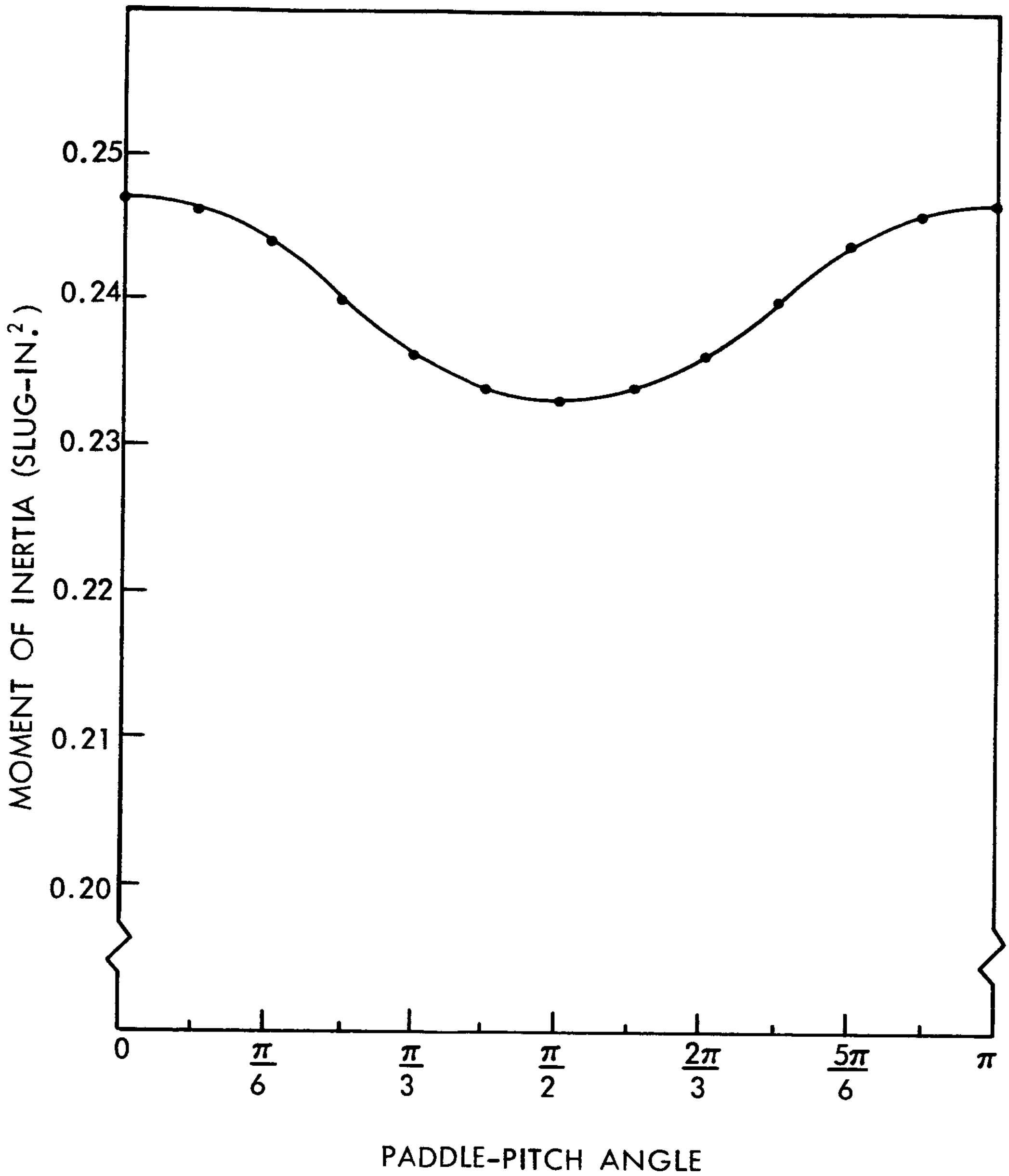

Figure 7. A plot of the moment of inertia versus pitch angle for the model paddle.